Isoform-specific Ras signaling is growth factor dependent.

Fiona E. Hood[1*], Bertram Klinger[2*], Anna U. Newlaczyl[1], Anja Sieber[2], Mathurin Dorel[2], Simon P. Oliver[3], Judy M. Coulson[1], Nils Blüthgen[2,4] and Ian A. Prior[1,4]

Running Title: Ras isoform-specific network topology

Keywords: RAS, network biology, systems biology, cancer

Character Count: 26,473

Competing interests: The authors have no competing financial interests to declare.

* These authors contributed equally to this study.

[1] Division of Cellular and Molecular Physiology, Institute of Translational Medicine, University of Liverpool, L69 3BX, UK.

[2] Institute of Pathology, Charité Universitätsmedizin Berlin, 10117 Berlin, Integrative Research Institute for the Life Sciences, Humboldt-Universität zu Berlin, 10099 Berlin, Institute for Theoretical Biology, Humboldt-Universität zu Berlin, 10115 Berlin, Germany.

[3] Department of Biological Sciences, University of Chester, CH1 4BJ, UK

[4] Corresponding Author: Ian A. Prior
Email: iprior@liv.ac.uk
Tel: +44-151-794-5332
Fax: +44-151-794-4434

[4] Corresponding Author: Nils Blüthgen
Email: nils.bluethgen@charite.de
Tel: +49-2093-8924

ABSTRACT

HRAS, NRAS and KRAS isoforms are almost identical proteins that are ubiquitously expressed and activate a common set of effectors. *In vivo* studies have revealed that they are not biologically redundant; however, the isoform-specificity of Ras signaling remains poorly understood. Using a novel panel of isogenic SW48 cell lines endogenously expressing wild type or G12V mutated activated Ras isoforms we have performed a detailed characterization of endogenous isoform-specific mutant Ras signaling. We find that despite displaying significant Ras activation, the downstream outputs of oncogenic Ras mutants are minimal in the absence of growth factor inputs. The lack of mutant KRAS-induced effector activation observed in SW48 cells appears to be representative of a broad panel of colon cancer cell lines harboring mutant KRAS. For MAP kinase pathway activation in KRAS mutant cells, the requirement for co-incident growth factor stimulation occurs at an early point in the Raf activation cycle. Finally, we find that Ras isoform-specific signaling was highly context dependent and did not conform to the dogma derived from ectopic expression studies.

INTRODUCTION

Ras proteins are ubiquitously expressed monomeric GTPases that represent key signaling hubs operating downstream of growth factor receptors to regulate cell proliferation, differentiation, protein synthesis, metabolism and cell survival (Pylayeva-Gupta *et al.*, 2011; Hobbs *et al.*, 2016). Activation of Ras generates a network response; however the most intensively studied effector pathways are the Raf-MEK-ERK and PtdIns 3-kinase (PI3K)-AKT pathways (Cox and Der, 2011). Oncogenic mutations in Ras at

codons 12, 13 or 61 are present in ~20% of human cancers (Prior *et al.*, 2012). Whilst all of these mutations are activating, recent work has indicated that each mutation specifies a distinct Ras output and propensity for promoting oncogenesis (De Roock *et al.*, 2010; Ihle *et al.*, 2012; Burd *et al.*, 2014; Alamo *et al.*, 2015; Hammond *et al.*, 2015; Stolze *et al.*, 2015; Winters *et al.*, 2017).

Three ubiquitously expressed Ras genes (HRAS, KRAS and NRAS) encode at least 4 isoforms that despite being almost identical are not functionally redundant. *In vivo* evidence for this comes from studies of mouse development where KRAS knockout mice are embryonic lethal whereas NRAS and HRAS double knockout mice are healthy (Koera *et al.*, 1997; Esteban *et al.*, 2001). Mice with HRAS inserted into the KRAS locus are viable; however, they exhibit cardiomyopathy that suggests that whilst the patterns of expression and gene dosing define the majority of the isoform-specific effects on development, there may still be KRAS-specific contributions to healthy development (Potenza *et al.*, 2005). Other evidence comes from large-scale profiling of the distribution of oncogenic Ras mutations that reveals an isoform-specific bias, with KRAS being the most frequently mutated isoform (Prior *et al.*, 2012). Furthermore, comparative studies using mouse models endogenously expressing activated mutant Ras isoforms reveal that only KRAS is capable of promoting colonic epithelium proliferation (Haigis *et al.*, 2008).

The Ras isoform-specific signaling differences underpinning these *in vivo* differences remain poorly understood. Ectopic over-expression studies revealed that whilst all Ras isoforms can activate canonical Raf-MAP-kinase and PtdIns 3-kinase (PI3K)-AKT pathways, they are differentially coupled. Specifically, KRAS is a better activator of Raf and Rac whereas HRAS and NRAS are better activators of PI3K (Yan *et al.*, 1998; Voice

94 *et al.*, 1999). Notably however, cells derived from KRAS mutant mouse models and
95 cancer cell lines harboring endogenous mutant Ras frequently do not exhibit the high
96 levels of PI3K and Raf-MAP kinase pathway activation seen in over-expression studies
97 (Iida *et al.*, 1999; Yip-Schneider *et al.*, 1999; Giehl *et al.*, 2000; Tuveson *et al.*, 2004;
98 Omerovic *et al.*, 2008). Similarly, synthetic lethality studies have illustrated the significant
99 context dependence associated with Ras signaling (Downward, 2015). This means that
100 any systematic characterization of isoform-specific Ras signaling needs to either be
101 based on very large panels of cell lines or performed in isogenic model systems where
102 endogenous signaling is measured.

103 Genome edited isogenic cell models allow the study of Ras variants expressed from
104 endogenous loci whilst avoiding context-dependent differences associated with different
105 genetic backgrounds. The majority of isogenic cell models have used genetic ablation of
106 a wild type or oncogenic KRAS allele resulting in some gene dosing differences between
107 wild type and oncogenic KRAS cells (Shirasawa *et al.*, 1993; Kim *et al.*, 2004; Di
108 Nicolantonio *et al.*, 2008; Yun *et al.*, 2009). More recently, recombinant adeno-associated
109 virus (rAAV) targeted genome editing has been used to generate a panel of isogenic
110 colorectal SW48 cells harboring a range of heterozygous mutations at codons 12 or 13
111 of the KRAS gene (De Roock *et al.*, 2010). Importantly, each individual mutation
112 generates a distinct oncogenic and network response (Ihle *et al.*, 2012; Burd *et al.*, 2014;
113 Hammond *et al.*, 2015); which means that any comparison of isoform-specific oncogenic
114 Ras signaling should incorporate the same activating mutation in each Ras gene. Taking
115 this into account we have developed a novel isogenic SW48 cell panel and employed a

focused network biology strategy to characterize the context-dependence of endogenous isoform-specific Ras signaling responses.

RESULTS

An isogenic panel of Ras G12V SW48 cells.

To investigate endogenous isoform-specific Ras signaling we generated isogenic $NRAS^{G12V}$ cell lines to complement an existing panel of heterozygous G12V mutated Ras variant SW48 cell lines. The same parental SW48 cells harboring wild type Ras isoforms and an rAAV-based genome editing strategy were used for the generation of all of the isogenic cell lines used in this study. The presence of an oncogenic Ras variant results in no obvious change in the protein abundance of the mutated or wild type Ras isoforms in each of the isogenic cell lines (Figure 1A). Highly transforming G12V mutations result in constitutive Ras activation and are present in 20% of human cancers that possess a mutated Ras (Prior *et al.*, 2012). However, the presence of a G12V mutated Ras isoform does not result in noticeable activation of canonical Ras effector pathways in the absence of serum where any signaling will be entirely contingent on the mutant Ras proteins (Figure 1B). The lack of response in serum-starved cells harbouring hyper-active Ras isoforms is in significant contrast to the effector activation observed in wild-type cells stimulated for 5 minutes with 15 ng/ml EGF (Figure 1B). One explanation for this could be that the absence of growth factors reduced nucleotide exchange on Ras to the point where G12V induced resistance to GAP-mediated GTP hydrolysis became redundant. However, this does not seem to be the case since significant Ras activity is detected for each isoform harboring a G12V mutation (Supplementary Figures 1A & 1B).

Standard cell culture conditions in the presence of 10% fetal bovine serum (FBS) revealed subtle isoform-specific patterns of effector activation, although they do not exceed the variability observed between $KRAS^{G12V}$ clones (Figure 1C). Therefore, mutant Ras activation of effectors is growth factor-dependent, and in the presence of a cocktail of growth factors in FBS we found no evidence for isoform specificity of endogenous Ras coupling to canonical effector pathways.

The variability in some outputs that we observed between the $KRAS^{G12V}$ cells raised questions about whether our other cells were likely to be representative. We were unable to generate additional $HRAS^{G12V}$ clones; however, we were able to generate a larger panel of $NRAS^{G12V}$ clones and observed similar MAPK pathway outputs to the clone that we had already selected and some heterogeneity in the AKT pathway response. (Supplementary Figure 2). The heterogeneity that we observed within the $NRAS^{G12V}$ panel was no greater than that observed between the $KRAS^{G12V}$ clones. Therefore, to acknowledge the potential for clonality to confound our observations we have included both $KRAS^{G12V}$ clones in all subsequent experiments. Although clonality means that any subtle differences between isoforms are unable to be clearly described, all clones show the same growth factor dependence for observing robust activation of canonical Ras effector pathways.

Basal downstream signaling is reduced and GF responses are isoform-specific.

To characterize the wider network responses of endogenous Ras isoform signaling we performed Luminex analysis incorporating phospho-antibody reporters of the activation status of 16 relevant downstream and feedback-regulated signaling nodes. Cells under

basal serum-starved cell culture conditions exhibited no activation of the Ras network in the presence of any of the constitutively active Ras isoforms (Supplementary Figure 3A). Indeed, all but 5 of the 64 measurements of Ras effector phosphorylation are decreased in mutant Ras cells versus wild type Ras Parental cells with both $KRAS^{G12V}$ clones generally displaying the most pronounced levels of Ras network suppression. This may reflect uncoupling of oncogenic Ras from downstream signaling and/or adaptive engagement of negative feedback pathways downstream of active Ras to suppress the network response.

In response to growth factor stimulation Parental as well as G12V mutant cell lines exhibit increased activation throughout their Ras network although this is context dependent (Figure 1D & Supplementary Figure 3B). Within the RAF-MAP kinase pathway the suppressed outputs in Ras mutant cells compared to Parental control are generally less evident with co-incident growth factor stimulation. This is particularly clear for all isoforms following EGF stimulation and for HGF stimulation of AKT in HRAS and KRAS mutant SW48 cells. EGF is the most potent of the three growth factors at activating the Raf pathway (pMEK-pERK-pp90RSK) with for example, 10-15-fold increases in MEK activation versus untreated, compared to 2-fold and 4-fold increases respectively following HGF and IGF stimulation (Figure 1D & Supplementary Figure 3B). In the EGF condition we also see a trend for an additive effect of HRAS for MEK-ERK activation. Whilst this suggests enhanced coupling between HRAS and the RAF-MAP kinase pathway compared to the other Ras isoforms, this is only present in the context of EGF stimulation and not a general feature of HRAS signaling. Notably, Ras activity is less

184 stimulatable by EGF if a cell harbors a mutant Ras isoform (Supplementary Figure 1A &
185 1C).
186 Within the PI3K pathway the significant suppression of KRAS activation of AKT and
187 RPS6 versus Parental control is lost when cells are stimulated with growth factors.
188 Strikingly, we observe potent activation of AKT and RPS6 in HGF-stimulated KRAS
189 mutant SW48 cells compared to the other cell lines (Figure 1D & Supplementary Figure
190 3B). Therefore, analogous to HRAS coupling to the RAF pathway, KRAS coupling to the
191 PI3K-AKT pathway is also highly context dependent and not a generic feature of
192 endogenous isoform-specific Ras signaling.
193
194 **Generation of perturbation data to systematically probe signaling.**
195 In order to get a deeper understanding, we used a network biology approach where
196 responses to pathway manipulations can be used to inform mathematical models that
197 predict signaling flow within a network (Klinger *et al.*, 2013). To generate the data for
198 mathematical modeling we performed, in addition to the stimulation experiments depicted
199 in Figure 1D, a broad range of combinatorial treatments targeting the Ras signaling
200 network (Figure 2A). Specifically, we stimulated the indicated isogenic SW48 cells for 20
201 minutes with empirically determined sub-saturating doses of three growth factors: EGF,
202 HGF and IGF. The cells had been pre-incubated for 1 hour with pharmacological inhibitors
203 of MEK, PI3K, MTOR, Src or solvent control and the phosphorylation status of 16
204 members of the local Ras signaling network was measured in a Luminex proteomics
205 platform (Figure 2B, Supplementary Figure 4). The presence of inhibitors was maintained
206 whilst co-incident growth factor stimulation was performed. The 20 minutes stimulatory

time point was chosen because it represented signaling in an approximate steady state during the long-term plateau phase that follows the initial strong transient peak (Klinger *et al.*, 2013).

Whilst generally there are subtle differences between cell lines in response to combinatorial treatments, AKT and MEK activation in HGF-stimulated KRAS cells are the most obvious outliers (Figure 2B, Supplementary Figure 4). All cell lines show >10-fold up-regulation of MEK phosphorylation in the presence of MEK inhibitor in EGF-stimulated cells that would be consistent with the loss of ERK–dependent negative feedback.

Modeling unveils subtle interlineal differences and a clear overall effect on signaling.

Luminex measurements were incorporated into mathematical models of network connectivity. We quantified the feed-forward and feedback relationships within a core network around Ras in each cell line using mathematical modeling. The algorithm determines network structure and parameterizations based on modular response analysis (MRA) (Klinger *et al.*, 2013) (Figure 3A). The model pipeline estimates response coefficients for an initial literature-based network and then iteratively edits the network to generate the best consensus network for the whole dataset derived from the perturbation experiments (Figure 3B point 1 to 2). Afterwards, significantly differing parameters across datasets are derived by first modeling all datasets with the same parameter set and then iteratively testing if individual fitting of each parameter significantly improved the overall fit (likelihood ratio test, $p \leq 0.05$). Of the 21 parameters tested 10 were required to be fitted specifically to each dataset. Looking at the localization of the edges where variability

was observed between the Ras mutant SW48 cells (Figure 3B, point 3) we can see that mainly the upstream signaling is different in the cell lines as 5 of the 6 receptor-associated parameters have to be differential whereas 8 of the 10 links downstream of ERK and AKT can be modeled with the same parameter (dashed links). When looking at the variation size of the differential signaling parameters across cell line models (as absolute coefficient of variation (CV)), 3 parameters (ERK-RAF feedback and MET downstream links) have to be varied strongly (CV > 1) whereas the remaining 7 only required minor changes (CV < 0.5). Thus, by individually modeling 10 of the total 24 parameters (including the 3 quantifications of inhibitor strengths that were not allowed to vary between cell lines) we can simulate cell-line specific responses that are in good agreement with the experimental data (Figure 3C). In order to more closely study the differential signaling, we clustered the cell lines according to the 10 variable parameters (row-wise normalized to absolute maximum; Figure 3D). Whilst most represent relatively subtle differences, in general the KRAS clones differentiate from the other cell lines across each of the parameters. The most striking differences are seen for HGF-induced activation of the RAF pathway and EGF/HGF/IGF-induced activation of the PI3K pathways that in each case is strongest in the KRAS mutant SW48 cells.

Apart from modeling individual Ras-isoform-specific models, we also applied a holistic model that included all datasets and modeled Ras mutations as perturbations of the Parental state. This allowed us to dissect the direct impact of the Ras mutation on their downstream outputs, using the previously defined network topology (see Figure 3B point 2). We found that all Ras mutations had a negative impact on signaling via PI3K and Raf versus Parental cells in each cellular context (Supplementary Figure 4). Specifically, we

find that basal signaling (in the absence of growth factors) is trending downwards in Ras mutant SW48 cell lines and their growth factor inducibility is decreased compared to Parental cells.

RAS^{G12V} signaling is attenuated upstream of RAF and requires receptor stimulation.

The network analysis reinforces our earlier observation that active Ras mutants do not exhibit potent effector stimulation in the absence of growth factors (Figure 1B), but the mechanism remains unclear. To address this, we focused on the Raf-MAP kinase pathway and considered each of the points where the signal could be interrupted or remodeled (Figure 4A). Phosphorylation of Ser259 on CRAF provides a 14-3-3 binding site that stabilizes CRAF in an auto-inhibited state unable to bind to Ras (Lavoie and Therrien, 2015). We observed a trend for reduced phosphorylation in the presence of growth factors but not RAS mutation alone (Figure 4B). The differences are marginal, and difficult to infer whether there will be consequences in the capacity for mutated RAS SW48 cells to recruit Raf to the membrane. However, Raf heterodimerization that occurs downstream of Ras recruitment was only seen in the presence of growth factor stimulation (Figure 4C). Oncogenically mutated KRAS was unable to promote Raf dimerization in the absence of growth factors suggesting either that Raf has not been efficiently recruited to the membrane or that dimerization is sensitive to co-incident growth factor signaling. Phosphorylation of Ser338 in the catalytic domain of CRAF indicates a fully active Raf molecule (Lavoie and Therrien, 2015). Clear growth factor dependence is seen for activating phosphorylation of CRAF and downstream effectors (Figure 4D & 4E). Finally,

we explored whether negative feedback was actively down-regulating mutant RAS signaling. Negative feedback phosphorylation of Ser289/296/301 on CRAF is mediated by activated ERK (Lavoie and Therrien, 2015), and we saw clear sensitivity of these sites to MEK inhibition following EGF stimulation but not in the starved condition when any MEK-ERK activation would be driven exclusively by mutant RAS (Figure 4F, Supplementary Figure 5). Therefore, the low levels of MEK-ERK phosphorylation seen in mutant RAS SW48 cells in the absence of growth factor stimulation are not a cause or consequence of negative feedback to CRAF. Together, these data demonstrate that oncogenically mutated RAS in our cells is unable to activate the Raf-MAP kinase pathway in the absence of co-incident growth factor stimulation and that the requirement for growth factors is evident from early in the Raf activation cycle.

Oncogenic Ras decoupling from effector pathways is also observed in a wider colorectal cancer cell panel.

There are no independent isogenic systems with equivalent mutations in each of Ras isoforms that we could use to increase confidence in the wider applicability of our findings. Instead we assembled a panel of colorectal cancer cell lines variously containing mutations in Ras pathway components (Figure 5A). Quantitation of Western blots from biological replicates reveals that KRAS mutation status does not define the effector response and co-clustering of mutant and wild-type KRAS cell lines is observed (Figure 5B). Notably, there is no evidence of effector stimulation in a subset of KRAS mutant cell lines with only 7/11 pMEK and 6/11 pAKT responses in KRAS mutant cells displaying increased phosphorylation versus wild type SW48 cells and only 1/11 KRAS mutant cell

lines showing strong pAKT increases (Figure 5A). This is consistent with the observations in the SW48 cell panel where the presence of mutated Ras did not lead to AKT or MEK phosphorylation in the serum-starved context (Figure 1B). We confirmed that the KRAS mutations are functional with all codon 12, 13 and 61 mutants exhibiting clear increases in KRAS activity compared to the wild type KRAS cell lines (Figure 5B). The A146T mutation that is observed in <0.05% of colon cancers had a negligible effect on LIM1215 cell KRAS activity. A lack of correlation between the amount of KRAS activity and effector activation is seen regardless of the presence or absence of co-incident mutations (Figure 5C). Similarly, in a wider Luminex-based analysis of Ras network activation we see that mutation status does not define the co-clustered responses, with the exception of pMEK responses in BRAF mutant cells (Figure 5D), and this data reemphasizes that cells with KRAS mutations show no general trend of increased signaling. In summary, data generated using the SW48 panel are consistent with a subset of colon cancer cell lines harboring mutant KRAS that also exhibit negligible effector activation in the absence of growth factors despite harboring activated KRAS.

DISCUSSION

Isoform-specific Ras signaling has been inferred from studies of mouse development and cancer mutation frequencies (Koera *et al.*, 1997; Esteban *et al.*, 2001; Prior *et al.*, 2012); however, we still only have a vague understanding of the isoform-specific mechanisms that may underpin this. Classic studies ectopically expressing Ras isoforms suggested clear differences in coupling of RAF and PI3K pathways to Ras isoforms (Yan *et al.*, 1998; Voice *et al.*, 1999; Hobbs *et al.*, 2016). Whilst amplification of Ras is observed

in some tumours, it is also true that over-expression can have distorting effects on signaling networks and senescence rather than an oncogenic program is observed in some Ras models (Sarkisian *et al.*, 2007). Isogenic cells provide a useful option for studying variants of endogenous signaling networks without being confounded by differences in the genetic backgrounds of the various cell lines. To date, isogenic cell-based studies have largely focused on comparative analysis of KRAS mutant versus wild type Ras cells (Vartanian *et al.*, 2013; Alamo *et al.*, 2015; Stolze *et al.*, 2015). Given the clear evidence for Ras mutation-specific signaling (Burd *et al.*, 2014; Hammond *et al.*, 2015; Winters *et al.*, 2017), we used the same G12V mutation in all three Ras isoforms. This novel cell line panel means that we have been able to perform the first analysis of endogenous isoform-specific Ras signaling in the same genetic background.

A notable initial observation was the general inability of G12V-mutated Ras isoforms to generate enhanced RAF and PI3K pathway signaling outputs compared to the wild type control (Figure 1B). G12V mutant Ras displays slow nucleotide exchange and slow GTP hydrolysis (Trahey *et al.*, 1987; Smith *et al.*, 2013), meaning that starvation and stimulation times could significantly influence the amount of active Ras in the cell. However, under the conditions in which we performed the experiments it was clear that the lack of effector activation was not due to a lack of Ras activation (Supplementary Figure 1A). It is relevant to note that SW48 cells harbor an $EGFR^{G719S}$ mutation that has been observed to promote ligand-independent EGFR kinase activity and Ras effector activation (Greulich *et al.*, 2005); and might be expected to exhibit pre-existing engagement of negative feedback pathways. However, we saw no evidence for this under our experimental conditions; all of the isogenic cell lines showed significant EGF

stimulatability, effector activation was minimal under serum-starved conditions and negative feedback was only consistently observed when EGF was added to cells (Supplementary Figure 5).

One potential criticism of our cell model is that the introduction of Ras oncogenic mutations into a wild type Ras SW48 cell parental background does not result in Ras addiction that is observed in some cancer cell lines in some contexts. Therefore, the signaling that we are observing may not be equivalent to “true” oncogenic mutant Ras signaling. In fact, DepMap analysis reveals that <30% of 2-D cultured KRAS mutant cell lines show strongly selective KRAS dependence (Tsherniak *et al.*, 2017). Furthermore, our observation of low levels of effector activation in Ras mutant SW48 cells has been seen before in a range of Ras mutant cancer cells and mouse models (Iida *et al.*, 1999; Yip-Schneider *et al.*, 1999; Giehl *et al.*, 2000; Tuveson *et al.*, 2004; Omerovic *et al.*, 2008; Vartanian *et al.*, 2013). We also observed a disconnect between the presence of activating KRAS or PIK3CA mutations and activation of their effector pathways in a panel of colon cancer cell lines commonly used to study KRAS and cancer biology (Figure 5). Our observations of Ras versus effector activation seen in the wild type and KRAS mutant SW48 cells sat well within the range of observations seen within the representative panel of colon cancer cell lines. Together, these argue against any exceptionalism for the isogenic SW48 model and the subtle effects on downstream signaling that are observed in the Ras mutant cells.

Importantly, studies across a wide range of Ras mutant cell models have usually not had access to an equivalent matched wild type Ras cell line for comparison so it has not generally been obvious that mutations that generate hyper-activated Ras can fail to result

in enhanced outputs compared to wild type Ras. It may be that the chronic trickle of low-level effector activation represents the reality of oncogenic signaling until the acquisition of genetic insults that further dysregulate signaling later in the progression of the cancer. Indeed, this low level signaling may be important for avoiding pushing the cells into cytotoxic stress, cell death or senescence (Varmus *et al.*, 2016).

Stimulation with growth factors potently activated Ras effectors (Figures 1 & 2); therefore, the lack of signaling seen in the Ras mutant cells was not due to a complete down-regulation or uncoupling of the Ras network. The second feature of the growth factor stimulation experiments was that Ras isoforms variably display enhanced coupling to the RAF and PI3K pathways (Figure 1D). However, these were not consistent across all growth factor stimulations (Figure 2) and the patterns did not conform to the observations seen in ectopic expression studies where KRAS preferentially coupled to Raf-MAP kinase and HRAS coupled to the PI3K pathway (Yan *et al.*, 1998; Voice *et al.*, 1999). Therefore, the dogma that Ras isoforms consistently favor coupling to a particular Ras pathway is incorrect in this endogenous context and the reality is far more nuanced and subject to growth factor modulation.

Mathematical modeling of the combinatorial treatment data revealed that the core signaling networks are very similar between the Ras isoforms (Figure 3). Nevertheless, there were some significant differences between the Ras isoforms that tended to distinguish the KRAS cell lines from the rest. The most pronounced of these differences were the increased GF-induced pathway activation (Figure 3D). HGF was particularly selective for KRAS-dependent PI3K pathway activation and this observation can be explained by the increased expression of the HGF receptor MET in KRAS mutant cell

391 lines including both G12V clones (Hammond *et al.*, 2015). Although MET is upstream of
392 KRAS, it has a well-established role in Ras-dependent tumorigenesis that typically
393 involves gene and protein amplification consistent with our observations (Webb *et al.*,
394 1998; Furge *et al.*, 2001; Xie *et al.*, 2012; Hammond *et al.*, 2015).

395 Importantly, the modeling did not point to a profound rewiring of the Ras network that
396 could explain the minimal effector activation in the absence of growth factors. Similarly,
397 our experiments to profile where the signaling downstream of Ras might be interrupted
398 revealed no evidence for network rewiring. Instead, they suggested that mutant Ras in
399 serum-starved cells was unable to efficiently activate Raf (Figure 4), arguing that growth
400 factor signaling is required to give competence to Ras activation of this key effector
401 pathway. Insufficiency may arise due to the coordinated regulation of kinases,
402 phosphatases, scaffolds and cofactors required for Raf-MAPK activation (Figure 4A)
403 (Lavoie and Therrien, 2015). In this context, growth factor receptor engagement of a wider
404 signaling network than Ras could be required to create a permissive state for efficient
405 Ras signaling. We note that ectopic expression studies have shown downstream
406 activation in serum-starved cells when Ras mutants are over-expressed (Yan *et al.*, 1998;
407 Voice *et al.*, 1999). Whilst this could argue against Ras insufficiency, an alternative
408 interpretation is that the higher concentration of Ras in cells is able to overcome the
409 requirement for growth factor signaling to prime the Ras network. Higher Ras
410 concentrations will influence the nanoscale organization of Ras on the plasma membrane
411 and increase the opportunity for dimerization and interactions with effectors (Zhou *et al.*,
412 2017). Alternative explanations for the requirement for growth factors could include a
413 requirement for SOS recruitment and wild type Ras engagement (Margarit *et al.*, 2003;

Jeng *et al.*, 2012), that alternative effectors may be preferentially bound in the absence of growth factors (Adhikari and Counter, 2018), or that nucleotide cycling within the Ras population may be required for efficient and disease-relevant signaling (Nichols *et al.*, 2018; Ruess *et al.*, 2018).

An important caveat with these studies is the use of a single isogenic cell model system and the potential for cell clonality to confound the observations. To give an indication of potential clonal heterogeneity we profiled a panel of NRAS clones to identify a representative clone (Supplementary Figure 2) and used more than one KRAS clone throughout our studies. Whilst it is clear that heterogeneity between clones exists, all of the clones conformed to the core observations of minimal effector responses to the presence of mutant Ras and similar substantial context-dependent responses to the presence of different growth factors. We also observe similar mutant KRAS-refractory responses in a representative panel of colon cancer cell lines. Whilst data from a single isogenic system is not definitive, our observations challenge current models and highlight fundamental aspects of Ras biology requiring further understanding.

In summary, we have created an isogenic cell panel that for the first time allows endogenous signaling of all Ras isoforms to be investigated in a common genetic background. The expression of isoform-specific G12V mutant Ras in the background of five wild type Ras alleles, all expressed in their native genomic contexts, represents the earliest stage of Ras-driven cancer. The observed limited activation of key effector pathways suggests that endogenous oncogenic Ras signaling relies on co-stimulatory events or further genetic perturbations to overcome cellular homeostasis mechanisms. These mechanisms are imposed at the earliest points in the effector activation cycle.

Differences between Ras isoform outputs were most clearly revealed with concomitant growth factor stimulation where it operated as a subtle but variable nudge on the significant growth factor-induced program. This is likely to be critical in the context of the tumour microenvironment where mutated Ras will operate in the presence of a cocktail of growth factors. Our systematic analysis reveals that the long-held view that Ras isoforms are consistently coupled to particular effector pathways is likely to be over simplistic and that the context dependence of HRAS, NRAS and KRAS signaling precludes any general predictions of likely pathway activation in response to a specific isoform.

MATERIALS AND METHODS

Reagents. The following inhibitors were used in various assays: AZD6244 (5μM; MEK; Selleck Chemicals), LY294002 (20μM; PI3K; Alexis Chemicals), Rapamycin (0.15μM; TOR; Selleck Chemicals), Dasatinib (25 nM; Src; Selleck Chemicals). The solvent control was DMSO (equal volume to each inhibitor). The following ligands were used (all Peprotech): IGF-1 (50 ng/ml), EGF (15 ng/ml) and HGF (50 ng/ml) with 0.1% BSA in PBS as solvent.

Cell lines. Ras mutation sequence verified isogenic SW48 cells were obtained from Horizon Discovery. The clones used were $HRAS^{G12V}$ (clone 1), $KRAS^{G12V}$ (clone c16 (K1) and clone c48 (K2)). Heterozygous knock-in of $NRAS^{G12V}$ (clone G9-1 (N1), clone 7-2 (N2), clone 4-2 (N3), and clone 8-1 (N4)) was generated from homozygous RAS^{WT} Parental SW48 cells, using AAV-mediated gene editing and sequence verified for the

presence of a heterozygous NRAS G12V mutation. SW48 cells were grown in McCoy's 5A media, supplemented with 10% [v/v] FBS, 100 units/ml penicillin and 100 µg/ml streptomycin (Thermo Fisher Scientific), at 37ºC in 5% [v/v] CO_2. The colon cancer cell panel comprising Caco-2, LIM1215, Colo205, Vaco432, RKO, SW837, Colo678, LS180, SW480, SW620, LoVo, T84, HCT8, HCT116, SW948 were cultured in DMEM (BE12-707F, Lonza/Biozym), supplemented with 1%Ultraglutamine (BE17-605E/U1, Lonza/Biozym), 100 units/ml penicillin and 100 µg/ml streptomycin (DE17-602E, Lonza/Biozym) and 10% [v/v] FBS (P30-1506, PAN Biotech) at 37°C and 5% CO2. Vaco432 cells were obtained from René Bernards lab (NKI), all other cell lines from AG Sers (Charité). All cell lines were Short tandem repeat (STR)-authenticated via Eurofins Genomics. Vaco432 could not be matched, as they were not found in the database. Mycoplasma testing was conducted by Eurofins Genomics.

Starvation of cells was done for 16h with FBS-free medium, before lysis. Lysis was done with the lysis Buffer from the Ras activation assay and protease inhibitors there included. For WB lysates, protease- and phosphatase inhibitors from Bio-Plex Cell Lysis Kit (Biorad ,171-304012) were used. Protein concentration was determined using BCA Protein Assay Kit (Pierce™,23227). After SDS-PAGE, proteins were blotted to nitrocellulose membranes and stained with Pierce™ Reversible Protein Stain Kit, wich was later used for normalisation. The following Abs were used: Rabbit anti-pMEK (CST9154), Rabbit anti-pAkt T308 (CST9275), Rabbit anti-pAkt S473 (CST4060), Rabbit anti-pERK (CST4370), Mouse anti-pERK (CST9106). The blots were imaged with Odyssey CLx and infrared labelled antibodies (all Li-Cor). Analysis was done using ImageJ after exporting pictures from ImageStudio (Li-Cor).

Luminex assays. Cell lysates were prepared using the Bio-Plex Pro™ Cell Signaling Reagent Kit (Bio-Rad), according to manufacturer's instructions. Briefly, cells seeded into 24 well plates were serum starved for 24 hours then incubated ±inhibitors in serum-free media for 1 hour, followed by a 20 minute stimulation ±growth factor in the continued presence of inhibitor. Lysates were measured with a Bio-Plex Protein Array (Bio-Rad, Hercules, CA) as described earlier (Klinger *et al.*, 2013) using magnetic bead-based ELISAs specific for phospho-AKT^{S473} (171-V50001M), phospho-c-Jun^{S63} (171-V50003M), phospho-EGFR^{Y1068} (171-V50004M), phospho-ERK1/2$^{T202,Y204/T185,Y187}$ (171-V50006M), phospho-GSK3A/B$^{S21/S9}$ (171-V50007M), phospho-IkBa^{S32,S36} (171-V50010M), phospho-JNK^{T183,Y185} (171-V50011M), phospho-MEK1^{S217,S221} (171-V50012M), phospho-mTOR^{S2448} (171-V50033M), phospho-p38^{T180,Y182} (171-V50014M), phospho-p53^{S15} (171-V50034M), phospho-PI3K^{Y458} (171-V50036M), phospho-RPS6^{S235,S236} (171-V50038M), phospho-p90RSK^{S380} (171-V50035M), phospho-SMAD2^{S465,S467} (171-V50019M) and phospho-Src^{T416} (171-V50039M). The capture antibody-coated beads as well as detection antibodies and the fluorescent conjugate SAPE were diluted 1:3. We used the R package lxb for data acquisition and normalized the data as described in Supplemental File 1. Statistical testing on excerpts of the luminex assay (i.e. Figure 1D, Supplementary Figure 3) was conducted by applying a one-way-ANOVA (analysis of variance) on logarithmized data of each subplot followed by multiple correction testing (Benjamini-Hochberg). For significant findings (FDR≤0.05) a post-hoc analysis was conducted (Tukey's Honestly Significant Difference test) to report adjusted p-values for the comparisons of interest.

Model construction and evaluation. The modeling procedure relies on a variant of modular response analysis (MRA) (Klinger *et al.*, 2013) that quantifies identifiable parameter (combinations) of a given network structure on base of systematic perturbation data. The network structure was derived from available literature and prior modelling approaches of colorectal cancer cell lines (Klinger *et al.*, 2013). Modeling was conducted in the two steps network structure determination and differential signaling detection: (1) Five cell line-specific models were generated based on the literature network choosing the best of 3×10^4 sample runs, observing that the ranked fits converged on the lower end and multiple best fits were found. These data sets were then locally adjusted to the data by determining superfluous links, i.e. removal did not significantly decrease the fit (likelihood-ratio test $p>0.05$), and missing links, i.e. addition, significantly improved the fit (Benjamini-Hochberg corrected $p \leq 0.05$) in all five cell lines. Among the extension candidates only those were included, for which a biological confirmation could be found in the literature (e.g. PI3K -> Raf). (2) The generated consensus network was then used to train a modelset (4×10^4 simulations) which models the individual data sets by a single parameter set. In order to determine significantly differing parameters, modelset parameters were iteratively relaxed to fit cell line-specific data (i.e. a split up of one parameter into five) in a greedy hill parameter splitting procedure with ensuing reverse lumping procedure (likelihood-ratio test $p \leq 0.05$, best of 10^3 simulations each).

The holistic model (Supplementary Figure 4) used the found consensus network above but treated Ras mutations as perturbations of the parental dataset, essentially modelling all datasets by one model with nodes of the Ras mutations added and each linked to RAF

and PI3K (10^5 simulations). The model was run on either the whole dataset or on datasets without stimulations. All modeling steps were conducted using the R package STASNet (Version 1.0.0) available under https://github.com/molsysbio/STASNet [38] as described in Supplemental File 2.

Ras activation assay and co-immunoprecipitation. Ras activity assays were performed as described using the Ras Activation Assay Kit (Cytoskeleton, BK008). Briefly, cells were serum starved for 24 hours, before incubation ±15 ng/ml EGF for 20 minutes, lysis and incubation of 300µg of pre-cleared lysate with 30 µl (100 µg) GST-Raf1-RBD-conjugated sepharose beads for 1 hour at 4 ˚C with rotation. Controls using serum-starved SW48 Parental cell lysates incubated with 1-3 mM GDP (100% inactive Ras), and 200 µM GTPγS (100% active Ras) were included for comparative normalisation of cell lines. For co-immunoprecipitation, cell lysates were prepared using NP40 lysis buffer (50 mM Tris-HCl, pH7.5, 150 mM NaCl, 1 % NP40 substitute protease inhibitor cocktail (P8465; Sigma), phosphatase inhibitor cocktail (PhosStop; Roche), 2 mM NaF). 1.5 mg lysate was pre-cleared with protein A-conjugated agarose (Sigma) then incubated with 2 µg BRAF antibody (Santa Cruz sc-5284) or normal mouse IgG Control (EMD Millipore, 12-371) and 7.5 µl (4.5 mg) Protein A agarose, for 2.5 hours. Beads from activity/co-precipitation experiments were washed and then boiled in sample buffer to elute proteins for loading on 4-12% NuPAGE Bis-Tris gels and visualisation by Western blotting. The following primary antibodies were used for Western blotting including for experiments measuring isoform-specific Ras activity; rabbit monoclonal pan-RAS (52939) phospho-CRAF^{S259} (173539; both AbCam), KRAS (Life Span Biosciences LS-C175665),

HRAS (sc-520), NRAS (sc-31), BRAF (sc5284), EGFR sc-03; all Santa Cruz), CRAF (9422), phospho-CRAF$^{S289/S296/S301}$ (9431), phospho-CRAF^{S338} (9427), MEK (9122), phospho-MEK$^{S217/S221}$ (9154), ERK (4695), phospho-ERK1/2$^{T202/Y204}$ (4370), AKT (9272), phospho-AKT^{S473} (4060), phospho-EGFR^{Y1068} (2234), actin (6276; all Cell Signaling Technology).

ACKNOWLEDGEMENTS

This work was supported by funding from NWCR (CR1025), the Wellcome Trust (WT092791) and by funding from BMBF, grants MapTorNet and ColoSys. We thank Rob Howes and Christine Schofield for help in generating the isogenic cell lines.

REFERENCES

Adhikari, H., and Counter, C.M. (2018). Interrogating the protein interactomes of RAS isoforms identifies PIP5K1A as a KRAS-specific vulnerability. Nature Communications *9*.

Alamo, P., Gallardo, A., Di Nicolantonio, F., Pavon, M.A., Casanova, I., Trias, M., Mangues, M.A., Lopez-Pousa, A., Villaverde, A., Vazquez, E., Bardelli, A., Cespedes, M.V., and Mangues, R. (2015). Higher metastatic efficiency of KRas G12V than KRas G13D in a colorectal cancer model. FASEB J *29*, 464-476.

Burd, C.E., Liu, W., Huynh, M.V., Waqas, M.A., Gillahan, J.E., Clark, K.S., Fu, K., Martin, B.L., Jeck, W.R., Souroullas, G.P., Darr, D.B., Zedek, D.C., Miley, M.J., Baguley, B.C., Campbell, S.L., and Sharpless, N.E. (2014). Mutation-specific RAS oncogenicity explains NRAS codon 61 selection in melanoma. Cancer Discov *4*, 1418-1429.

Cox, A.D., and Der, C.J. (2011). Ras history: The saga continues. Small Gtpases *1*, 2-27.

De Roock, W., Jonker, D.J., Di Nicolantonio, F., Sartore-Bianchi, A., Tu, D., Siena, S., Lamba, S., Arena, S., Frattini, M., Piessevaux, H., Van Cutsem, E., O'Callaghan, C.J., Khambata-Ford, S., Zalcberg, J.R., Simes, J., Karapetis, C.S., Bardelli, A., and Tejpar, S. (2010). Association of KRAS p.G13D mutation with outcome in patients with

chemotherapy-refractory metastatic colorectal cancer treated with cetuximab. Jama *304*, 1812-1820.

Di Nicolantonio, F., Arena, S., Gallicchio, M., Zecchin, D., Martini, M., Flonta, S.E., Stella, G.M., Lamba, S., Cancelliere, C., Russo, M., Geuna, M., Appendino, G., Fantozzi, R., Medico, E., and Bardelli, A. (2008). Replacement of normal with mutant alleles in the genome of normal human cells unveils mutation-specific drug responses. Proc Natl Acad Sci U S A *105*, 20864-20869.

Downward, J. (2015). RAS Synthetic Lethal Screens Revisited: Still Seeking the Elusive Prize? Clin Cancer Res *21*, 1802-1809.

Esteban, L.M., Vicario-Abejon, C., Fernandez-Salguero, P., Fernandez-Medarde, A., Swaminathan, N., Yienger, K., Lopez, E., Malumbres, M., McKay, R., Ward, J.M., Pellicer, A., and Santos, E. (2001). Targeted genomic disruption of H-ras and N-ras, individually or in combination, reveals the dispensability of both loci for mouse growth and development. Mol Cell Biol *21*, 1444-1452.

Furge, K.A., Kiewlich, D., Le, P., Vo, M.N., Faure, M., Howlett, A.R., Lipson, K.E., Woude, G.F., and Webb, C.P. (2001). Suppression of Ras-mediated tumorigenicity and metastasis through inhibition of the Met receptor tyrosine kinase. Proc Natl Acad Sci U S A *98*, 10722-10727.

Giehl, K., Skripczynski, B., Mansard, A., Menke, A., and Gierschik, P. (2000). Growth factor-dependent activation of the Ras-Raf-MEK-MAPK pathway in the human pancreatic carcinoma cell line PANC-1 carrying activated K-ras: implications for cell proliferation and cell migration. Oncogene *19*, 2930-2942.

Greulich, H., Chen, T.H., Feng, W., Janne, P.A., Alvarez, J.V., Zappaterra, M., Bulmer, S.E., Frank, D.A., Hahn, W.C., Sellers, W.R., and Meyerson, M. (2005). Oncogenic transformation by inhibitor-sensitive and -resistant EGFR mutants. Plos Med *2*, 1167-1176.

Haigis, K.M., Kendall, K.R., Wang, Y., Cheung, A., Haigis, M.C., Glickman, J.N., Niwa-Kawakita, M., Sweet-Cordero, A., Sebolt-Leopold, J., Shannon, K.M., Settleman, J., Giovannini, M., and Jacks, T. (2008). Differential effects of oncogenic K-Ras and N-Ras on proliferation, differentiation and tumor progression in the colon. Nat Genet *40*, 600-608.

611 Hammond, D.E., Mageean, C.J., Rusilowicz, E.V., Wickenden, J.A., Clague, M.J., and
612 Prior, I.A. (2015). Differential reprogramming of isogenic colorectal cancer cells by distinct
613 activating KRAS mutations. J Proteome Res *14*, 1535-1546.
614 Hobbs, G.A., Der, C.J., and Rossman, K.L. (2016). RAS isoforms and mutations in cancer
615 at a glance. Journal of Cell Science *129*, 1287-1292.
616 Ihle, N.T., Byers, L.A., Kim, E.S., Saintigny, P., Lee, J.J., Blumenschein, G.R., Tsao, A.,
617 Liu, S.Y., Larsen, J.E., Wang, J., Diao, L.X., Coombes, K.R., Chen, L., Zhang, S.X.,
618 Abdelmelek, M.F., Tang, X.M., Papadimitrakopoulou, V., Minna, J.D., Lippman, S.M.,
619 Hong, W.K., Herbst, R.S., Wistuba, I.I., Heymach, J.V., and Powis, G. (2012). Effect of
620 KRAS Oncogene Substitutions on Protein Behavior: Implications for Signaling and
621 Clinical Outcome. J Natl Cancer I *104*, 228-239.
622 Iida, M., Towatari, M., Nakao, A., Iida, H., Kiyoi, H., Nakano, Y., Tanimoto, M., Saito, H.,
623 and Naoe, T. (1999). Lack of constitutive activation of MAP kinase pathway in human
624 acute myeloid leukemia cells with N-Ras mutation. Leukemia *13*, 585-589.
625 Jeng, H.H., Taylor, L.J., and Bar-Sagi, D. (2012). Sos-mediated cross-activation of wild-
626 type Ras by oncogenic Ras is essential for tumorigenesis. Nature Communications *3*.
627 Kim, J.S., Lee, C., Foxworth, A., and Waldman, T. (2004). B-Raf is dispensable for K-
628 Ras-mediated oncogenesis in human cancer cells. Cancer Res *64*, 1932-1937.
629 Klinger, B., Sieber, A., Fritsche-Guenther, R., Witzel, F., Berry, L., Schumacher, D., Yan,
630 Y., Durek, P., Merchant, M., Schafer, R., Sers, C., and Bluthgen, N. (2013). Network
631 quantification of EGFR signaling unveils potential for targeted combination therapy. Mol
632 Syst Biol *9*, 673.
633 Koera, K., Nakamura, K., Nakao, K., Miyoshi, J., Toyoshima, K., Hatta, T., Otani, H., Aiba,
634 A., and Katsuki, M. (1997). K-ras is essential for the development of the mouse embryo.
635 Oncogene *15*, 1151-1159.
636 Lavoie, H., and Therrien, M. (2015). Regulation of RAF protein kinases in ERK signalling.
637 Nat Rev Mol Cell Bio *16*, 281-298.
638 Margarit, S.M., Sondermann, H., Hall, B.E., Nagar, B., Hoelz, A., Pirruccello, M., Bar-
639 Sagi, D., and Kuriyan, J. (2003). Structural evidence for feedback activation by Ras-GTP
640 of the Ras-specific nucleotide exchange factor SOS. Cell *112*, 685-695.

Nichols, R.J., Haderk, F., Stahlhut, C., Schulze, C.J., Hemmati, G., Wildes, D., Tzitzilonis, C., Mordec, K., Marquez, A., Romero, J., Hsieh, T., Zaman, A., Olivas, V., McCoach, C., Blakely, C.M., Wang, Z.P., Kiss, G., Koltun, E.S., Gill, A.L., Singh, M., Goldsmith, M.A., Smith, J.A.M., and Bivona, T.G. (2018). RAS nucleotide cycling underlies the SHP2 phosphatase dependence of mutant BRAF-, NF1-and RAS-driven cancers. Nature Cell Biology *20*, 1064-1073.

Omerovic, J., Hammond, D.E., Clague, M.J., and Prior, I.A. (2008). Ras isoform abundance and signalling in human cancer cell lines. Oncogene *27*, 2754-2762.

Potenza, N., Vecchione, C., Notte, A., De Rienzo, A., Rosica, A., Bauer, L., Affuso, A., De Felice, M., Russo, T., Poulet, R., Cifelli, G., De Vita, G., Lembo, G., and Di Lauro, R. (2005). Replacement of K-Ras with H-Ras supports normal embryonic development despite inducing cardiovascular pathology in adult mice. EMBO Rep *6*, 432-437.

Prior, I.A., Lewis, P.D., and Mattos, C. (2012). A comprehensive survey of Ras mutations in cancer. Cancer Res *72*, 2457-2467.

Pylayeva-Gupta, Y., Grabocka, E., and Bar-Sagi, D. (2011). RAS oncogenes: weaving a tumorigenic web. Nat Rev Cancer *11*, 761-774.

Ruess, D.A., Heynen, G.J., Ciecielski, K.J., Ai, J.Y., Berninger, A., Kabacaoglu, D., Gorgulu, K., Dantes, Z., Wormann, S.M., Diakopoulos, K.N., Karpathaki, A.F., Kowalska, M., Kaya-Aksoy, E., Song, L., van der Laan, E.A.Z., Lopez-Alberca, M.P., Nazare, M., Reichert, M., Saur, D., Erkan, M.M., Hopt, U.T., Sainz, B., Birchmeier, W., Schmid, R.M., Lesina, M., and Algul, H. (2018). Mutant KRAS-driven cancers depend on PTPN11/SHP2 phosphatase. Nat Med *24*, 954-960.

Sarkisian, C.J., Keister, B.A., Stairs, D.B., Boxer, R.B., Moody, S.E., and Chodosh, L.A. (2007). Dose-dependent oncogene-induced senescence in vivo and its evasion during mammary tumorigenesis. Nat Cell Biol *9*, 493-505.

Shirasawa, S., Furuse, M., Yokoyama, N., and Sasazuki, T. (1993). Altered growth of human colon cancer cell lines disrupted at activated Ki-ras. Science *260*, 85-88.

Smith, M.J., Neel, B.G., and Ikura, M. (2013). NMR-based functional profiling of RASopathies and oncogenic RAS mutations. P Natl Acad Sci USA *110*, 4574-4579.

Stolze, B., Reinhart, S., Bulllinger, L., Frohling, S., and Scholl, C. (2015). Comparative analysis of KRAS codon 12, 13, 18, 61, and 117 mutations using human MCF10A isogenic cell lines. Sci Rep *5*, 8535.

Trahey, M., Milley, R.J., Cole, G.E., Innis, M., Paterson, H., Marshall, C.J., Hall, A., and McCormick, F. (1987). Biochemical and biological properties of the human N-ras p21 protein. Mol Cell Biol *7*, 541-544.

Tsherniak, A., Vazquez, F., Montgomery, P.G., Weir, B.A., Kryukov, G., Cowley, G.S., Gill, S., Harrington, W.F., Pantel, S., Krill-Burger, J.M., Meyers, R.M., Ali, L., Goodale, A., Lee, Y., Jiang, G., Hsiao, J., Gerath, W.F.J., Howell, S., Merkel, E., Ghandi, M., Garraway, L.A., Root, D.E., Golub, T.R., Boehm, J.S., and Hahn, W.C. (2017). Defining a Cancer Dependency Map. Cell *170*, 564-576 e516.

Tuveson, D.A., Shaw, A.T., Willis, N.A., Silver, D.P., Jackson, E.L., Chang, S., Mercer, K.L., Grochow, R., Hock, H., Crowley, D., Hingorani, S.R., Zaks, T., King, C., Jacobetz, M.A., Wang, L., Bronson, R.T., Orkin, S.H., DePinho, R.A., and Jacks, T. (2004). Endogenous oncogenic K-ras(G12D) stimulates proliferation and widespread neoplastic and developmental defects. Cancer Cell *5*, 375-387.

Varmus, H., Unni, A.M., and Lockwood, W.W. (2016). How Cancer Genomics Drives Cancer Biology: Does Synthetic Lethality Explain Mutually Exclusive Oncogenic Mutations? Cold Spring Harb Symp Quant Biol *81*, 247-255.

Vartanian, S., Bentley, C., Brauer, M.J., Li, L., Shirasawa, S., Sasazuki, T., Kim, J.S., Haverty, P., Stawiski, E., Modrusan, Z., Waldman, T., and Stokoe, D. (2013). Identification of mutant KRas-dependent phenotypes using a panel of isogenic cell lines. J Biol Chem *288*, 2403-2413.

Voice, J.K., Klemke, R.L., Le, A., and Jackson, J.H. (1999). Four human ras homologs differ in their abilities to activate Raf-1, induce transformation, and stimulate cell motility. J Biol Chem *274*, 17164-17170.

Webb, C.P., Taylor, G.A., Jeffers, M., Fiscella, M., Oskarsson, M., Resau, J.H., and Vande Woude, G.F. (1998). Evidence for a role of Met-HGF/SF during Ras-mediated tumorigenesis/metastasis. Oncogene *17*, 2019-2025.

Winters, I.P., Chiou, S.H., Paulk, N.K., McFarland, C.D., Lalgudi, P.V., Ma, R.K., Lisowski, L., Connolly, A.J., Petrov, D.A., Kay, M.A., and Winslow, M.M. (2017). Multiplexed in vivo

homology-directed repair and tumor barcoding enables parallel quantification of Kras variant oncogenicity. Nat Commun *8*, 2053.

Xie, T., G, D.A., Lamb, J.R., Martin, E., Wang, K., Tejpar, S., Delorenzi, M., Bosman, F.T., Roth, A.D., Yan, P., Bougel, S., Di Narzo, A.F., Popovici, V., Budinska, E., Mao, M., Weinrich, S.L., Rejto, P.A., and Hodgson, J.G. (2012). A comprehensive characterization of genome-wide copy number aberrations in colorectal cancer reveals novel oncogenes and patterns of alterations. PLoS One *7*, e42001.

Yan, J., Roy, S., Apolloni, A., Lane, A., and Hancock, J.F. (1998). Ras isoforms vary in their ability to activate Raf-1 and phosphoinositide 3-kinase. J Biol Chem *273*, 24052-24056.

Yip-Schneider, M.T., Lin, A., Barnard, D., Sweeney, C.J., and Marshall, M.S. (1999). Lack of elevated MAP kinase (Erk) activity in pancreatic carcinomas despite oncogenic K-ras expression. Int J Oncol *15*, 271-279.

Yun, J., Rago, C., Cheong, I., Pagliarini, R., Angenendt, P., Rajagopalan, H., Schmidt, K., Willson, J.K., Markowitz, S., Zhou, S., Diaz, L.A., Jr., Velculescu, V.E., Lengauer, C., Kinzler, K.W., Vogelstein, B., and Papadopoulos, N. (2009). Glucose deprivation contributes to the development of KRAS pathway mutations in tumor cells. Science *325*, 1555-1559.

Zhou, Y., Prakash, P., Gorfe, A.A., and Hancock, J.F. (2017). Ras and the Plasma Membrane: A Complicated Relationship. Cold Spring Harb Perspect Med *8*, pii:a031831.

FIGURE LEGENDS

Figure 1. *Context-dependent activation of canonical Ras effectors by endogenous Ras isoforms.* (A) Ras isoform protein expression is similar to Parental (P) control in all isogenic cell lines. (B) The presence of an oncogenic Ras^{G12V} allele is insufficient to activate effector pathways in the absence of co-incident growth factor stimulation. (C) There are no clear isoform-specific effects on effector activation in response to cell culture in the presence of 10% FBS. Western blotting data representative of n≥3 biological replicates. (D) Luminex-based measurement of key nodes within the Ras signaling network in untreated and growth factor-stimulated cells reveals that differential coupling of Ras isoforms with the RAF (pMEK, pERK, pp90RSK) or PI3K PI3K (pAKT, pMTOR, pRPS6) pathways is not a generic feature of Ras signaling; mean ±SD of n=2 biological replicates. p-values correspond to Tukey's test (versus Parental) for those cases where multiple testing corrected one-way-ANOVA was significant (FDR≤0.05); * $p<0.05$, **, $p<0.01$, *** $p<0.001$.

Figure 2. *Generation of systematic perturbation data.* (A) Schema depicting stimulated, inhibited and measured nodes within the Ras signaling network that were used for generation of systematic perturbation data. (B) Log_2-fold changes (FC) of phosphorylation in response to combinations of growth factor stimulation and node inhibition across the 5 isogenic SW48 cells lines measured with Luminex-based phospho-assays are displayed. Values are averaged signals from n=2 biological replicates normalized to the untreated Parental cell line control (BSA treated control lane).

Figure 3. *Model fit reveals Ras isoform-specific differences in network topology.* (A) Workflow of modeling steps to determine differential signaling based on Modular Response Analysis (MRA). (B) Realization of modeling steps from A: the starting network, consensus network with pruned (red) and extended (blue) links (chi^2-test, $p \leq 0.05$) and the resultant differential signaling network of which the numbers and line width reflect differential signaling across the five cell lines as absolute coefficient of variation (CV) of the parameter quantifications and dashed links denote unvaried links. (C) Side-by-side comparison of experimental data (black) and model simulations (yellow) derived from the final model (step 3 in B). (D) Clustered heatmap of the variable network parameters with each row scaled by the absolute maximal value.

Figure 4. *Oncogenically mutated Ras requires co-incident growth factor stimulation to activate Raf.* (A) The Raf activation cycle. (B) RAF auto-inhibitory phosphorylation is largely unchanged by Ras mutation. (C) Growth factor dependence is observed with BRAF:CRAF heterodimerization, (D) Activating phosphorylation of the CRAF kinase catalytic domain, (E) downstream activation of CRAF effectors, and (F) ERK-mediated negative feedback to CRAF revealed by decreased CRAF phosphorylation in the presence of MEK inhibitors. All blots are representative of $n \geq 3$ biological replicates. Graphs depict mean values ±SEM; paired, equal variance t-test versus Parental cells or indicated pair-wise comparisons, * $p<0.05$, ** $p<0.01$, *** $p<0.001$, $n=3$ biological replicates. Cells starved for 24 hours (EGF -), ±15ng/ml EGF stimulation (EGF +) for 5 minutes for all experiments except 20 minutes for feedback experiment.

Figure 5. *Ras effector activation does not correlate with KRAS mutation status in a panel of colon cancer cells.* (A) Mutation status of a representative panel of colorectal cancer cell lines. Representative Western blots from n=2-4 biological replicates indicate that the presence of an oncogenic mutation is not necessarily leading to activation of effector pathways in the absence of co-incident growth factor stimulation. (B) Quantification of KRAS activity measured using a Raf RBD assay (see (A) for representative blot) indicates that codon 12, 13 and 61 mutant cells contain activated KRAS (mean ± SEM; n=3). (C) KRAS activity does not correlate with ERK and AKT phosphorylation. (D) Luminex-based measurement of key nodes within the Ras signaling network reveals that responses do not strictly co-cluster based on mutation status. Values are averaged signals from n=2-6 biological replicates normalized to the SW48 cells. In all experiments, cells were starved for 16 hours prior to assaying.

Supplementary Figure 1. *Oncogenic Ras is active in the absence of growth factor stimulation.* (A) Ras activity in isogenic SW48 cells measured using a Raf RBD assay. GDP represents 100% inactive Ras and GTPγS indicates 100% active Ras. (B) Quantification of Ras activity (n=3) indicates that all G12V mutated isoforms are significantly activated versus wild type control cells. (C) Mutated Ras isoforms display impaired responsiveness to EGF stimulation. Western blot data are representative of n=3 experiments. Graphs depict mean values ±SEM; paired t-test, * $p<0.05$, ** $p<0.01$.

Supplementary Figure 2. *Profiling Ras signaling in available SW48 cell G12V Ras clones.* Evidence for some clonality is seen with $KRAS^{G12V}$ cells. In contrast, the Ras

792 signaling outputs from $NRAS^{G12V}$ clones are largely homogenous. Cells were grown
793 under standard cell culture conditions in the presence of 10% FBS. Western blotting data
794 representative of n=4-7 biological replicates. Graphs of quantified Western blots depict
795 mean values ±SEM; paired t-test, * $p<0.05$.
796
797 **Supplementary Figure 3.** *Luminex measurement of Ras network outputs in the panel of*
798 *isogenic SW48 cells.* (A) Luminex analysis of Ras signaling pathway nodes reveals a lack
799 of network activation versus the Parental control in serum-starved isogenic SW48 cells.
800 Data points from technical and biological replicates are shown (circles), bars represent
801 mean ± SD from n=2 experiments each comprising n=3-8 technical replicates. (B) An
802 alternative presentation of data from Figure 1D with data grouped by cell line. Data points
803 indicating n=2 biological replicates. p-values correspond to Tukey's test (for A versus
804 Parental, for B versus untreated) for those cases where multiple testing corrected one-
805 way-ANOVA was significant (FDR≤0.05); * $p<0.05$, **, $p<0.01$, *** $p<0.001$.
806
807 **Supplementary Figure 4.** *An alternative presentation of a subset of data from Figure 2B*
808 *grouped by cell line.*
809
810 **Supplementary Figure 5.** *Parameter heatmap where Ras mutations are modeled as*
811 *perturbations.* All mutations exert a negative influence on signaling. In the presence (all
812 data) and absence of growth factors (no GF). Basal signaling versus wild type Ras cells
813 trends downwards for both PI3K and RAF pathways for all isoforms and shows no clear

814 differential isoform-specific effect on downstream outputs (for modeling details refer to
815 Material and Methods and Supplemental File 2).
816
817 **Supplementary Figure 6.** *ERK-dependent negative feedback to CRAF is independent*
818 *of the presence of oncogenic Ras mutants.* Blots are from a single experiment and
819 representative of n=3 biological replicates. Graphs depict mean values ±SEM; n=3; paired
820 t-test versus Parental cells or indicated pair-wise comparisons, * $p<0.05$, ** $p<0.01$, ***
821 $p<0.001$. Cells starved for 24 hours, ± 15ng/ml EGF stimulation for 20 minutes, ±5μM
822 AZD6244 MEK inhibitor, 60 minutes pre-treatment and co-incident incubation during the
823 EGF stimulation.
824
825
826 **Supplementary File 1.** *SW48 Ras isoforms: Normalization.* Code for normalizing plate
827 to plate variability and pre- and post-normalization data.
828
829 **Supplementary File 2.** *Modelling workflow.* Code and workthrough of the modeling steps
830 for network structure determination.
831
832 **Supplementary File 3.** *Ras activity screen.* Colorectal cell line panel signaling readout
833 analysis html containing source data.
834
835
836
837

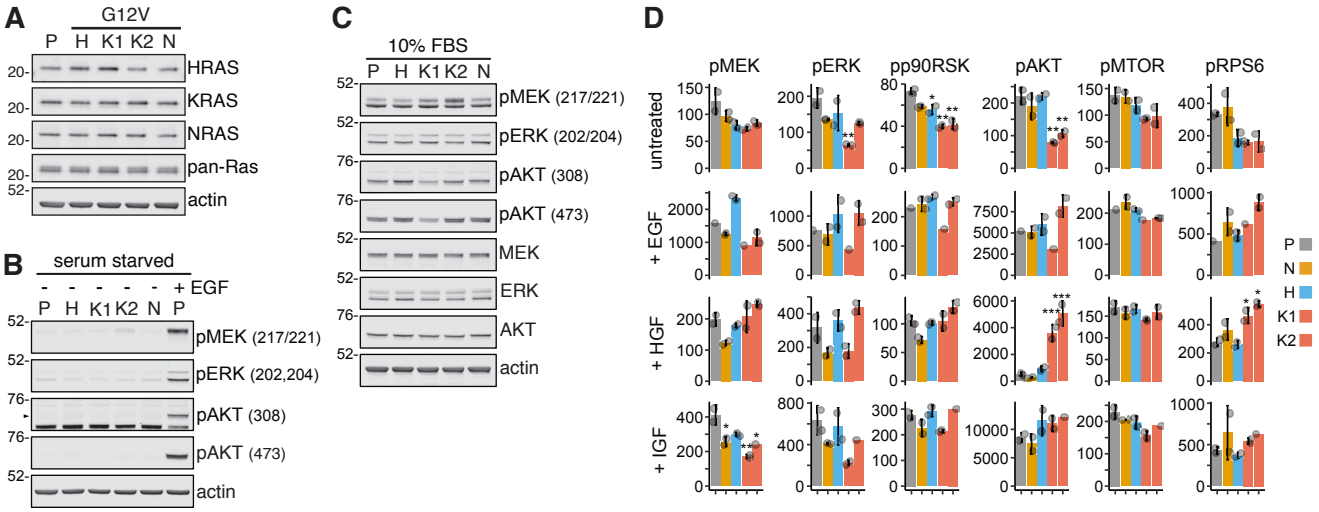
A
G12V
P H K1 K2 N
20-
HRAS
KRAS
NRAS
pan-Ras
52-
actin
B
serum starved
- - - - - + EGF
P H K1 K2 N P
52-
pMEK (217/221)
pERK (202,204)
76-
pAKT (308)
pAKT (473)
actin
C
10% FBS
P H K1 K2 N
pMEK (217/221)
pERK (202/204)
pAKT (308)
pAKT (473)
MEK
ERK
AKT
actin
D
pMEK
pERK
pp90RSK
pAKT
pMTOR
pRPS6
untreated
+ EGF
+ HGF
+ IGF
P
N
H
K1
K2

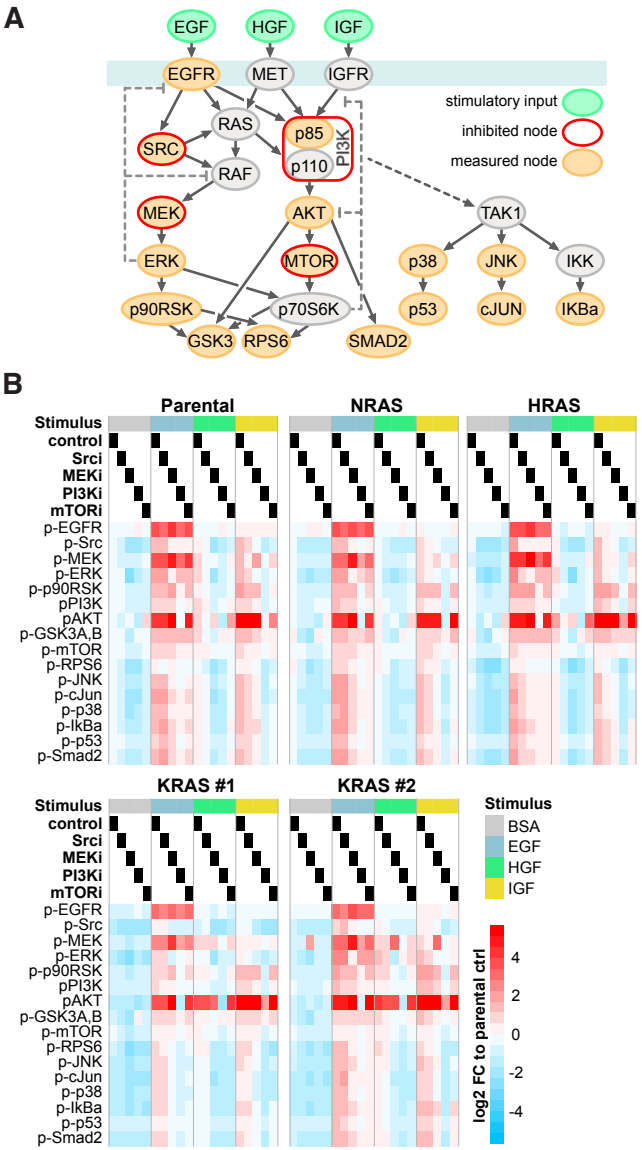
A
EGF
HGF
IGF
EGFR
MET
IGFR
stimulatory input
inhibited node
measured node
RAS
p85
PI3K
SRC
p110
RAF
MEK
AKT
TAK1
ERK
MTOR
p38
JNK
IKK
p90RSK
p70S6K
p53
cJUN
IKBa
GSK3
RPS6
SMAD2
B
Parental
NRAS
HRAS
Stimulus
control
Srci
MEKi
PI3Ki
mTORi
p-EGFR
p-Src
p-MEK
p-ERK
p-p90RSK
pPI3K
pAKT
p-GSK3A,B
p-mTOR
p-RPS6
p-JNK
p-cJun
p-p38
p-IkBa
p-p53
p-Smad2
KRAS #1
KRAS #2
Stimulus
BSA
EGF
HGF
IGF
log2 FC to parental ctrl
4
2
0
-2
-4

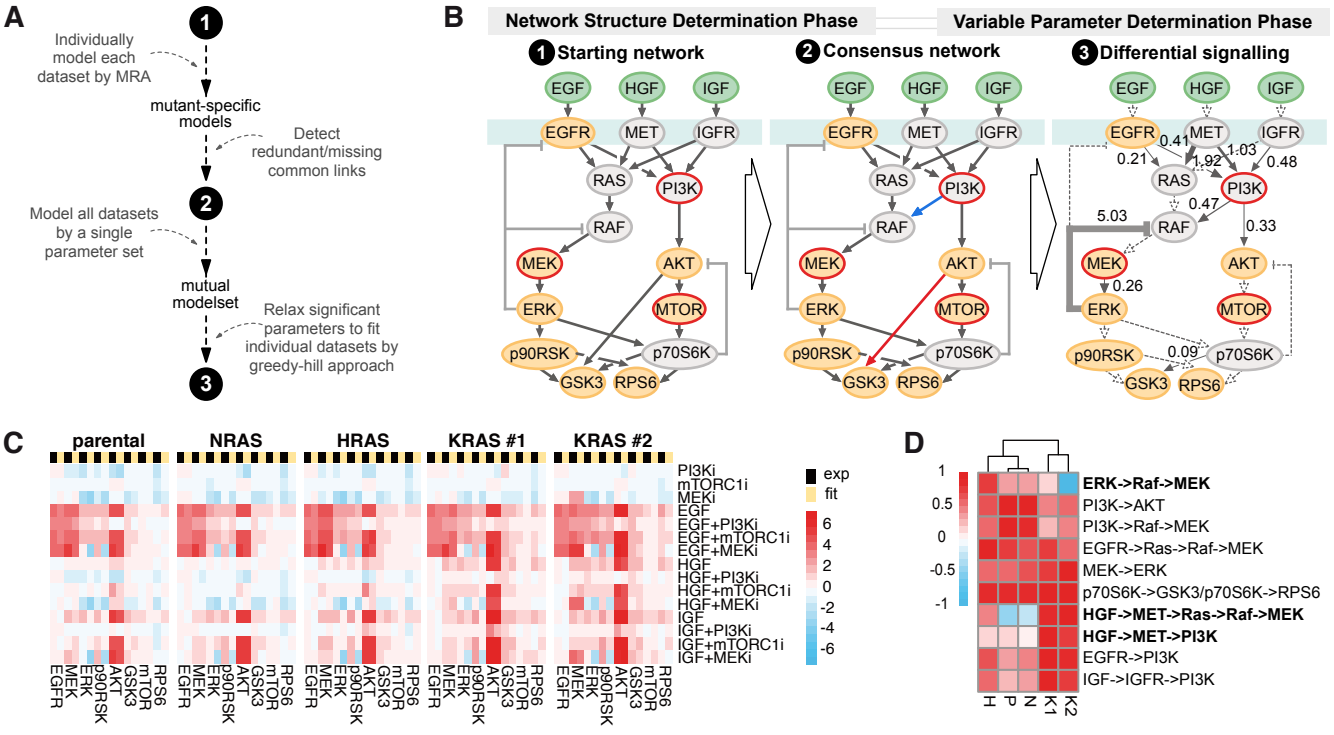
A
Individually model each dataset by MRA
mutant-specific models
Detect redundant/missing common links
Model all datasets by a single parameter set
mutual modelset
Relax significant parameters to fit individual datasets by greedy-hill approach
B
Network Structure Determination Phase
Variable Parameter Determination Phase
1 Starting network
2 Consensus network
3 Differential signalling
EGF
HGF
IGF
EGFR
MET
IGFR
RAS
PI3K
RAF
MEK
AKT
ERK
MTOR
p90RSK
p70S6K
GSK3
RPS6
0.41
1.03
0.21
1.92
0.48
0.47
5.03
0.33
0.26
0.09
C
parental
NRAS
HRAS
KRAS #1
KRAS #2
PI3Ki
mTORC1i
MEKi
EGF
EGF+PI3Ki
EGF+mTORC1i
EGF+MEKi
HGF
HGF+PI3Ki
HGF+mTORC1i
HGF+MEKi
IGF
IGF+PI3Ki
IGF+mTORC1i
IGF+MEKi
exp
fit
6
4
2
0
-2
-4
-6
EGFR
MEK
ERK
p90RSK
AKT
GSK3
mTOR
RPS6
D
1
0.5
0
-0.5
-1
ERK->Raf->MEK
PI3K->AKT
PI3K->Raf->MEK
EGFR->Ras->Raf->MEK
MEK->ERK
p70S6K->GSK3/p70S6K->RPS6
HGF->MET->Ras->Raf->MEK
HGF->MET->PI3K
EGFR->PI3K
IGF->IGFR->PI3K
H
P
N
K1
K2

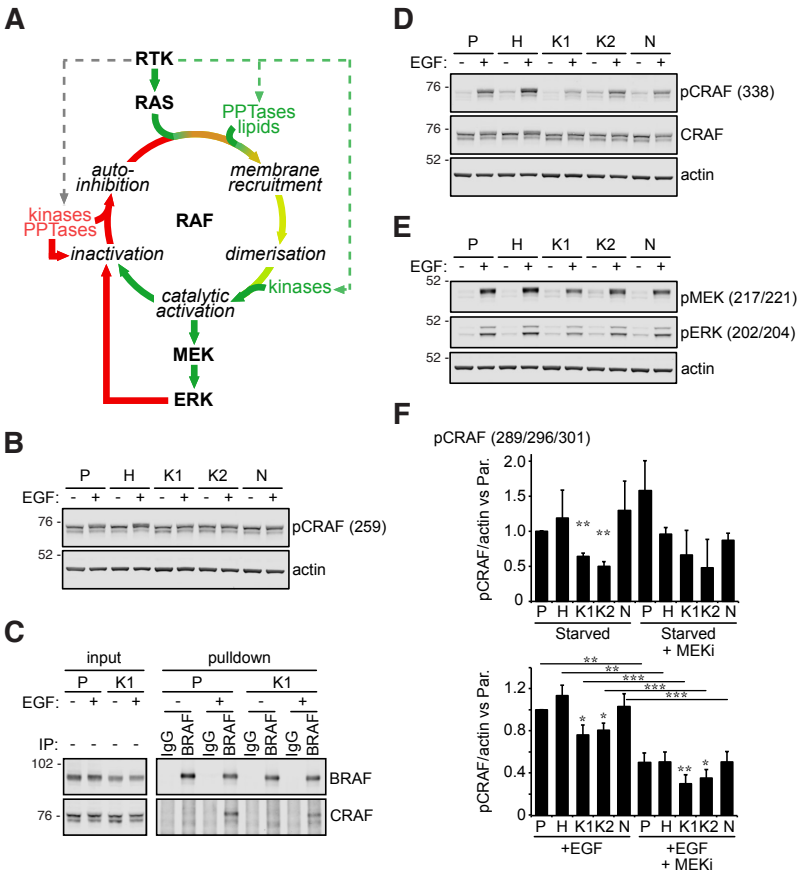
A
RTK
RAS
PPTases
lipids
auto-
inhibition
membrane
recruitment
kinases
PPTases
RAF
inactivation
dimerisation
kinases
catalytic
activation
MEK
ERK
B
P H K1 K2 N
EGF: - + - + - + - + - +
76
pCRAF (259)
52
actin
C
input
pulldown
P K1
P K1
EGF: - + - +
- + - +
IP: - - - -
IgG BRAF IgG BRAF IgG BRAF IgG BRAF
102
BRAF
76
CRAF
D
P H K1 K2 N
EGF: - + - + - + - + - +
76
pCRAF (338)
76
CRAF
52
actin
E
P H K1 K2 N
EGF: - + - + - + - + - +
52
pMEK (217/221)
52
pERK (202/204)
52
actin
F
pCRAF (289/296/301)
pCRAF/actin vs Par.
2.0
1.5
1.0
0.5
0
**
**
P H K1 K2 N P H K1 K2 N
Starved
Starved
+ MEKi
pCRAF/actin vs Par.
1.2
0.8
0.4
0
**
**
***
***
***
*
*
**
*
P H K1 K2 N P H K1 K2 N
+EGF
+EGF
+ MEKi

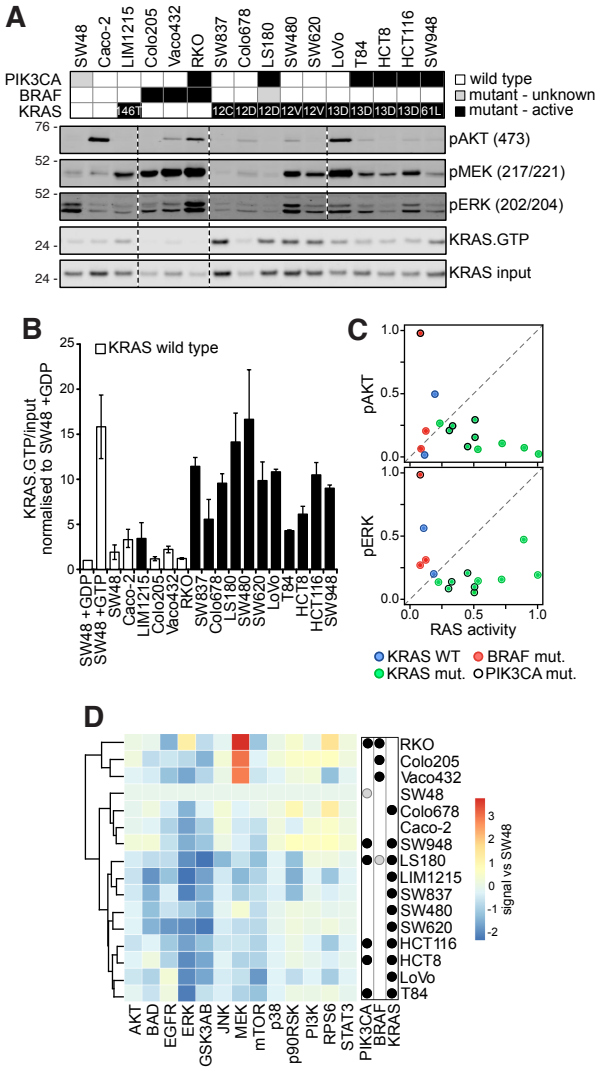
A
SW48
Caco-2
LIM1215
Colo205
Vaco432
RKO
SW837
Colo678
LS180
SW480
SW620
LoVo
T84
HCT8
HCT116
SW948
PIK3CA
BRAF
KRAS
146T
12C
12D
12D
12V
12V
13D
13D
13D
13D
61L
wild type
mutant - unknown
mutant - active
76
52
52
24
24
pAKT (473)
pMEK (217/221)
pERK (202/204)
KRAS.GTP
KRAS input
B
KRAS wild type
KRAS.GTP/input
normalised to SW48 +GDP
25
20
15
10
5
0
SW48 +GDP
SW48 +GTP
SW48
Caco-2
LIM1215
Colo205
Vaco432
RKO
SW837
Colo678
LS180
SW480
SW620
LoVo
T84
HCT8
HCT116
SW948
C
pAKT
pERK
1.0
0.5
0.0
RAS activity
KRAS WT
BRAF mut.
KRAS mut.
PIK3CA mut.
D
RKO
Colo205
Vaco432
SW48
Colo678
Caco-2
SW948
LS180
LIM1215
SW837
SW480
SW620
HCT116
HCT8
LoVo
T84
signal vs SW48
3
2
1
0
-1
-2
AKT
BAD
EGFR
ERK
GSK3AB
JNK
MEK
mTOR
p38
p90RSK
PI3K
RPS6
STAT3
PIK3CA
BRAF
KRAS

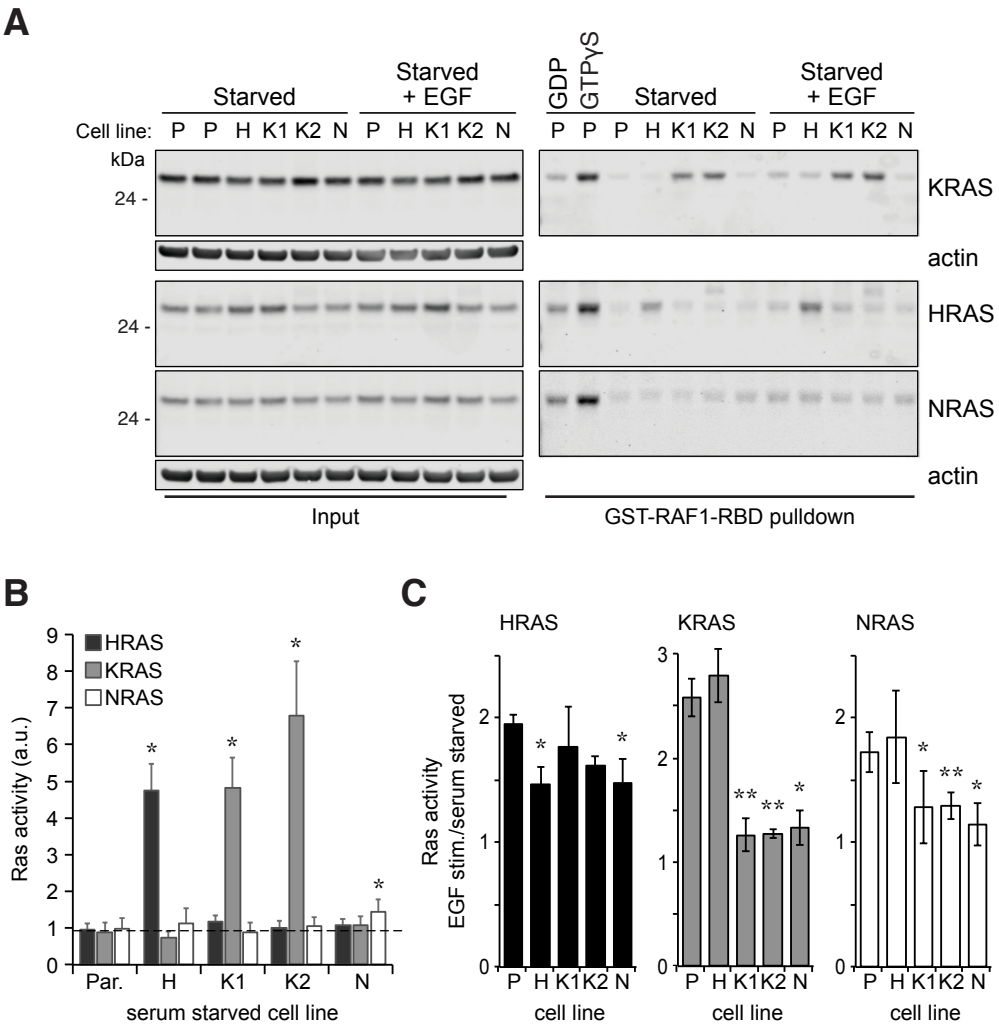
A
Starved
Starved + EGF
GDP
GTPγS
Starved
Starved + EGF
Cell line: P P H K1 K2 N P H K1 K2 N P P P H K1 K2 N P H K1 K2 N
kDa
24 -
KRAS
actin
HRAS
NRAS
Input
GST-RAF1-RBD pulldown
B
HRAS
KRAS
NRAS
Ras activity (a.u.)
Par. H K1 K2 N
serum starved cell line
C
HRAS
KRAS
NRAS
Ras activity
EGF stim./serum starved
P H K1 K2 N
cell line

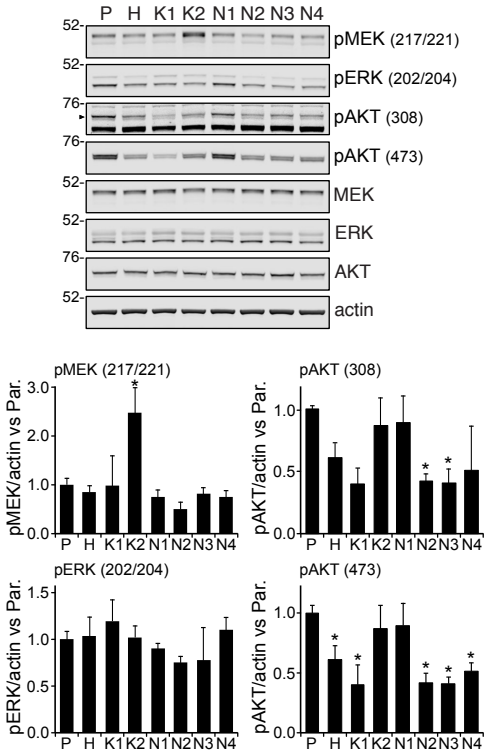
P H K1 K2 N1 N2 N3 N4
52-
pMEK (217/221)
52-
pERK (202/204)
76-
pAKT (308)
76-
pAKT (473)
52-
MEK
52-
ERK
76-
AKT
52-
actin
pMEK (217/221)
pMEK/actin vs Par.
3.0
2.0
1.0
0.0
pAKT (308)
pAKT/actin vs Par.
1.0
0.5
0.0
pERK (202/204)
pERK/actin vs Par.
1.5
1.0
0.5
0.0
pAKT (473)
pAKT/actin vs Par.
1.0
0.5
0.0
P H K1 K2 N1 N2 N3 N4

A

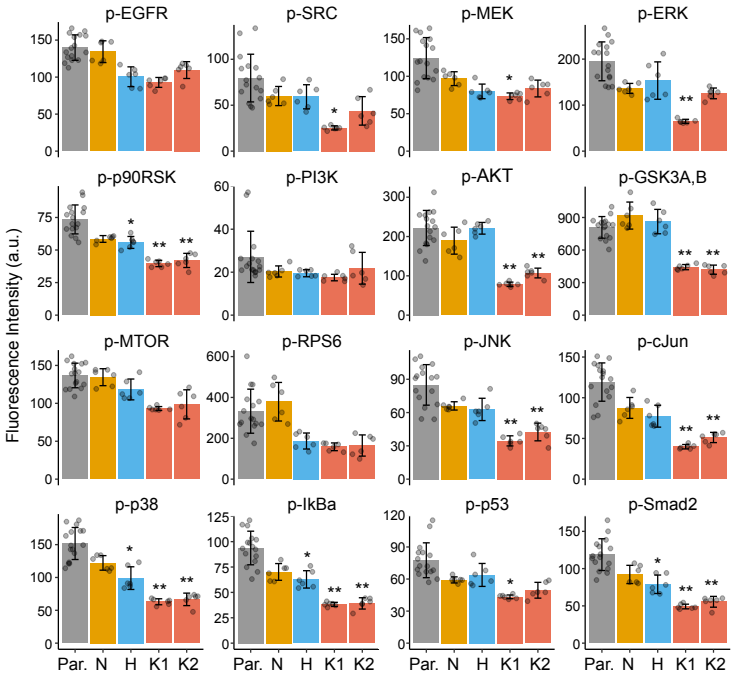
p-EGFR
p-SRC
p-MEK
p-ERK
p-p90RSK
p-PI3K
p-AKT
p-GSK3A,B
p-MTOR
p-RPS6
p-JNK
p-cJun
p-p38
p-IkBa
p-p53
p-Smad2
Fluorescence Intensity (a.u.)
Par. N H K1 K2

B

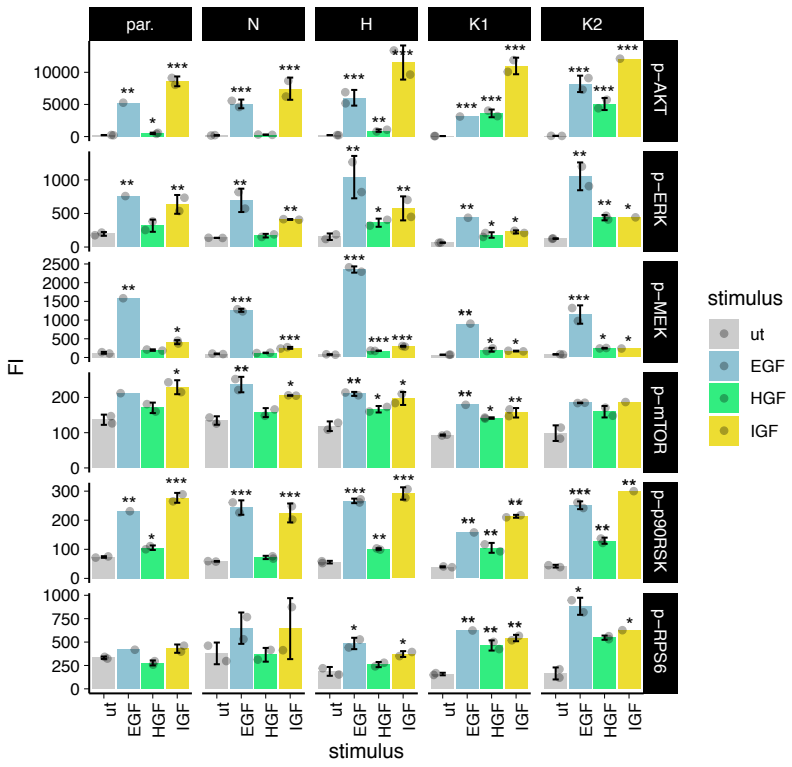
par.
N
H
K1
K2
p-AKT
p-ERK
p-MEK
p-mTOR
p-p90RSK
p-RPS6
FI
ut EGF HGF IGF
stimulus
stimulus
ut
EGF
HGF
IGF

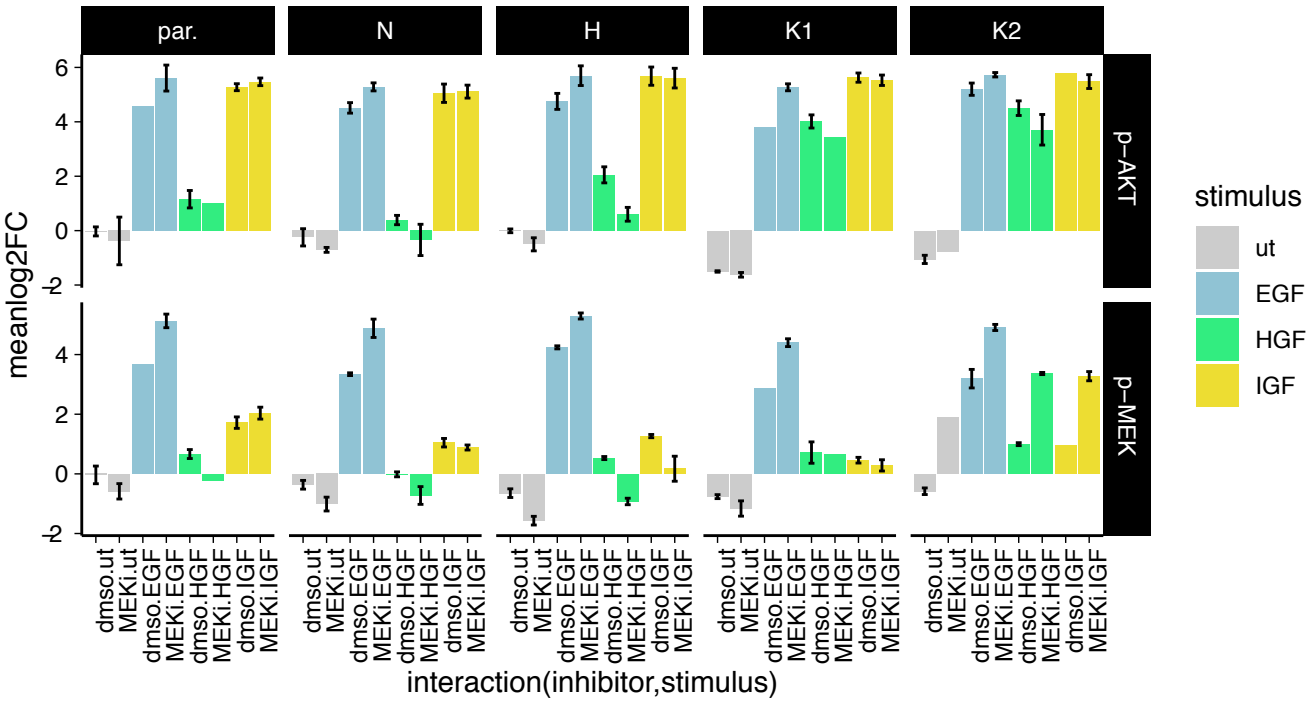
par.
N
H
K1
K2
p−AKT
p−MEK
meanlog2FC
6
4
2
0
−2
dmso.ut
MEKi.ut
dmso.EGF
MEKi.EGF
dmso.HGF
MEKi.HGF
dmso.IGF
MEKi.IGF
interaction(inhibitor,stimulus)
stimulus
ut
EGF
HGF
IGF

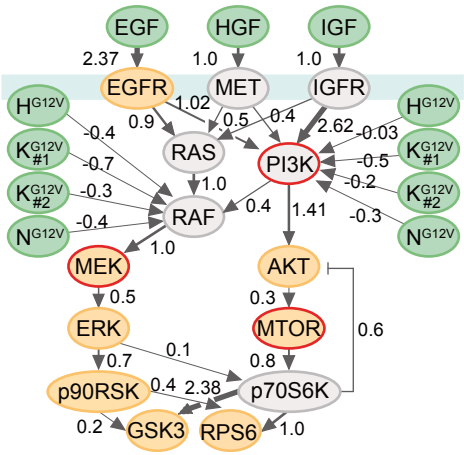
EGF
HGF
IGF
2.37
1.0
1.0
EGFR
MET
IGFR
H G12V
K G12V #1
K G12V #2
N G12V
1.02
0.9
0.5
0.4
2.62
0.03
-0.4
-0.7
-0.3
-0.4
RAS
PI3K
RAF
1.0
0.4
1.41
-0.5
-0.2
-0.3
1.0
MEK
AKT
0.5
0.3
ERK
MTOR
0.6
0.1
0.7
0.8
p90RSK
p70S6K
0.4
2.38
0.2
GSK3
RPS6
1.0

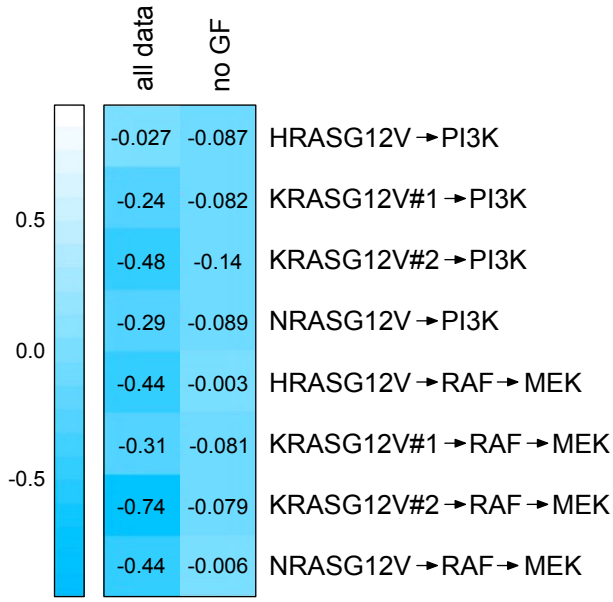
all data
no GF
0.5
0.0
-0.5
-0.027
-0.087
HRASG12V → PI3K
-0.24
-0.082
KRASG12V#1 → PI3K
-0.48
-0.14
KRASG12V#2 → PI3K
-0.29
-0.089
NRASG12V → PI3K
-0.44
-0.003
HRASG12V → RAF → MEK
-0.31
-0.081
KRASG12V#1 → RAF → MEK
-0.74
-0.079
KRASG12V#2 → RAF → MEK
-0.44
-0.006
NRASG12V → RAF → MEK

ERK-RAF negative feedback phosphorylation